Elijah Garner
John Deere, Inc.

Roderic Lakes
Department of Engineering Physics and
Department of Biomedical Engineering,
University of Wisconsin—Madison,
147 ERB, 1500 Engineering Dr.,
Madison, WI 53706-1687
e-mail: lakes@engr.wisc.edu

Taeyong Lee
Department of Biomedical Engineering,
University of Wisconsin—Madison,
147 ERB, 1500 Engineering Dr.,
Madison, WI 53706-1687

Colby Swan
Department of Civil and Environmental
Engineering,
University of Iowa,
Iowa City, IA 52242

Richard Brand
Department of Orthopaedic Surgery,
University of Iowa,
Iowa City, IA 52242

Viscoelastic Dissipation in Compact Bone: Implications for Stress-Induced Fluid Flow in Bone

Viscoelastic properties of wet and dry human compact bone were studied in torsion and in bending for both the longitudinal and transverse directions at frequencies from 5 mHz to 5 kHz in bending to more than 50 kHz in torsion. Two series of tests were done for different longitudinal and transverse specimens from a human tibia. Wet bone exhibited a larger viscoelastic damping tan δ (phase between stress and strain sinusoids) than dry bone over a broad range of frequency. All the results had in common a relative minimum in tan δ over a frequency range, 1 to 100 Hz, which is predominantly contained in normal activities. This behavior is inconsistent with an optimal ''design'' for bone as a shock absorber. There was no definitive damping peak in the range of frequencies explored, which could be attributed to fluid flow in the porosity of bone. [S0148-0731(00)00102-3]

1 Introduction

1.1 Bone Viscoelastic Properties. Viscoelasticity includes phenomena such as creep, relaxation, and dynamic response. The loss angle δ is the phase angle between stress and strain during oscillatory (dynamic) loading. Dynamic viscoelasticity is referred to as internal friction, and recoverable viscoelasticity as anelasticity. Viscoelasticity in bone has been known since Rauber [1] studied creep as well as anisotropy and strength of bone.

Viscoelastic damping in bone as quantified by the loss tangent, tan δ, is intermediate between that of polymers and metals. Polymers exhibit values from 0.1 in the glassy state to 1 or more in the glass–rubber transition. In structural metals such as steel, brass, and aluminum, viscoelastic effects are usually small: tan δ is 10^{-3} or less; as small as 3.6×10^{-6} for some aluminum alloys. Compact bone, at physiological frequencies from 0.1 to 10 Hz, exhibits tan δ on the order 0.01 to 0.02, intermediate between values seen in metals and polymers. In Fig. 1, results in shear obtained by several authors are combined. Observe that the loss tangent in shear of wet compact bone attains a broad *minimum* over the frequency range associated with most bodily activities. Here, different kinds of bone are compared since no one experimental modality covered a sufficient portion of the time or frequency scale. Also shown in Fig. 1 is a Debye peak (Eq. (2)) in tan δ, corresponding, by Fourier transformation, to a single exponential (Eq. (1)) in the creep or relaxation behavior, and corresponding to a three element spring-dashpot model. Observe that the loss tangent of bone occupies a much larger region of the frequency domain than a Debye peak.

Contributed by the Bioengineering Division for publication in the JOURNAL OF BIOMECHANICAL ENGINEERING. Manuscript received by the Bioengineering Division March 9, 1999; revised manuscript received November 30, 1999. Associate Technical Editor: T. M. Keaveny.

1.2 Structure and Causal Mechanisms. Viscoelasticity in bone arises from a variety of mechanisms. Since bone is a hierarchical composite, which contains structure at multiple length scales, viscoelasticity can arise from multiple processes at the different scales. On the molecular scale, collagen as a proteinaceous phase can give rise to significant viscoelasticity [2]. The similarity of *shape* of the relaxation curves for bone and demineralized bone as obtained by Sasaki et al. [2] is suggestive of a major role for collagen over the time scale studied. The following caveat suggests itself. At a grosser scale, there are also many *interfaces* such as the cement lines between osteons (which are large, 200-μm-dia, hollow fibers), and the boundaries between lamellae within osteons, in bone. A thin layer of a protein-polysaccharide substance occurs at cement line interfaces. Cement lines are compliant [3]. Viscous-like cement line motion gives rise to a portion of the viscoelasticity in bone, particularly at long times [4]. The mineral phase of bone is crystalline hydroxyapatite, which is virtually elastic; it provides the stiffness of bone. Thermoelastic coupling is a causal mechanism in which damping arises from stress-induced heat flow from the material to its environment or between different heterogeneities in the material. Thermoelastic damping from heat flow between osteons may account for some of the damping between 0.01 Hz and 10 Hz [5,6]. Damping from lamellae of an osteon would occur at higher frequency due to their smaller scale. The magnitude of thermoelastic damping depends on the degree of heterogeneity, but that is not well known. Piezoelectric coupling was considered as a damping mechanism by Lakes and Katz [5,6], but was judged to have a negligible contribution to the damping of bone.

Viscoelasticity can also result from fluid flow in porous media [7], including hard tissue such as bone [5,6] and soft tissue such as cardiac muscle [8] and spinal disks. Stress-induced fluid flow can be explored indirectly via the viscoelastic effects that occur as a

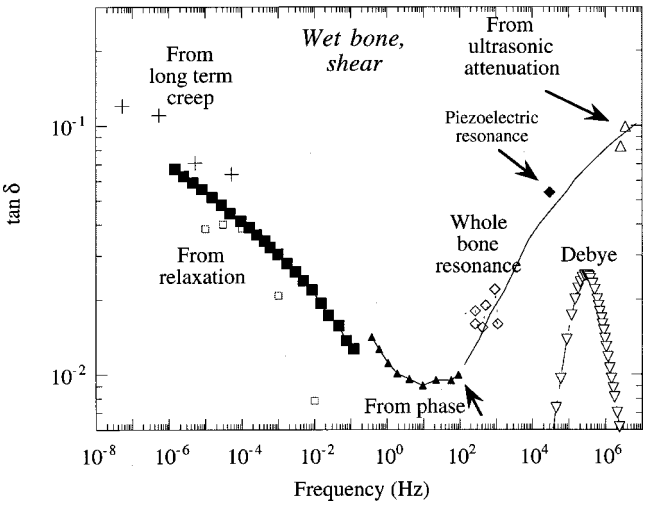

Fig. 1 tan δ for human compact bone, adapted from data of Lakes et al. [29] for wet human tibial bone at 37°C (calculated from relaxation, solid squares, ■; directly measured, ▲), from curve fit of Sasaki et al. [2] to data for wet bovine femoral bone (open squares, □). Also shown are results of Thompson [42] for whole dog radius at acoustic frequencies (diamond, ◇), of wet human femoral bone by Lakes [43] via a piezoelectric ultrasonic oscillator (diamonds, ♦), and of Adler and Cook [44] at ultrasonic frequency for canine bone at room temperature (open triangles, △). Damping at low frequency inferred from long-term creep by Park and Lakes [45], plus +. For comparison, a Debye peak is shown (inverted triangles ∇). the peak can occur at any frequency, depending on the material.

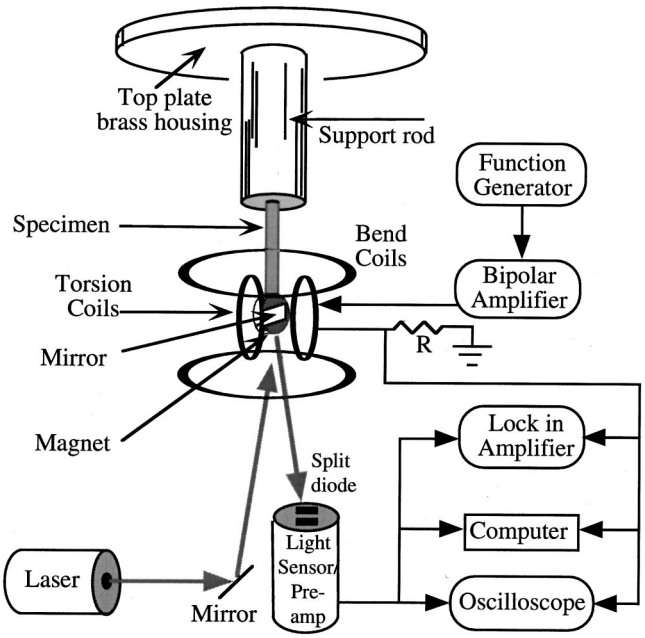

Fig. 2 Experimental configuration, the instrument uses electromagnetic force from the Helmholtz coil upon the end magnet to generate torque, and a measurement of the deflection of a reflected laser beam to determine end angular displacement. High frequencies are attainable since the measurement system contains little inertia.

result. An indirect approach is appropriate for bone since it would be difficult to measure fluid flow directly in the small voids within bone. Fluid flow in bone is of particular interest since it is a hypothetical stimulus for bone remodeling [9–12].

It is the purpose of the present study to examine experimentally the viscoelasticity of wet and dry cortical bone in the longitudinal and transverse directions in both bending and torsion over a wide range of frequency. The aim is to elucidate causal mechanisms, specifically fluid flow. Bending and torsion responses are compared since the volume change that occurs in bending is expected to give rise to a damping peak due to fluid flow in the Haversian systems. Wet and dry are compared since only fully hydrated bone can give rise to a damping peak due to fluid flow. Longitudinal and transverse directions are also explored since the anisotropy in bone's permeability and the orientation of Haversian and other canals could give rise to differences in time constants and damping magnitudes associated with fluid flow.

2 Materials and Methods

2.1 Viscoelastic Experiment. Viscoelastic measurements were performed in torsion at ambient temperature using an apparatus developed by Chen and Lakes [13] and refined by Brodt et al. [14]. The wide frequency range, up to 11 decades of time and frequency, is obtained by eliminating resonances from the devices used for loading and for displacement measurement, by minimizing the inertia attached to the specimen, and by use of a geometry giving rise to a simple specimen resonance structure amenable to simple analysis. Higher frequencies (1 kHz to 100 kHz) became accessible following design modifications permitting study of higher harmonic modes [15]. The rationale for such a method is that bone and other composites do not obey time-temperature superposition. In some polymers that obey superposition, one can infer material properties over a wider range of frequency from test results taken at different temperatures.

Torque (sinusoidal for dynamic studies and step function for creep studies) was produced electromagnetically by a Helmholtz coil acting upon a high-intensity neodymium iron boron magnet at the free end of the cylindrical bone specimen. Angular displacement of the free end was measured via laser light reflected from a small mirror upon the magnet to a split-diode light detector. Torsion was achieved by applying current to the vertical coil shown in Fig. 2. Bending moments were applied by applying current to the horizontal coil. Bending deformation was detected by inserting a Dove prism into the light beam path to change direction of the beam motion from vertical to horizontal. The phase angle φ between torque and angular displacement was measured using an SR850 digital lock-in amplifier with a claimed phase resolution of 0.001 deg corresponding to $\tan\delta = 1.75\times10^{-5}$. Actual phase resolution was limited by noise. Phase resolution was less than the size of the data points in the graphs, except at the lower frequencies, where noise was problematical; there resolution was about 10^{-3}. Data reduction was conducted using the relationship for the torsional rigidity of a viscoelastic cylinder with an attached mass at one end and fixed at the other end.

For the present data of relatively low loss near the first resonance, it was sufficient to treat the bone cylinder and magnet as a single-degree-of-freedom oscillator to obtain δ, the material phase angle, from φ, the structural phase angle, in the subresonant region. The lumped relations are as follows: $|G^*| = G'\sqrt{1+\tan^2\delta}$ and $\tan\delta = \tan\varphi(1-(v/v_0)^2)$. Here, v_0 is the first natural frequency and v is frequency. G' is the storage shear modulus (a measure of stiffness), the real part of the complex dynamic shear modulus G^*. Moduli were inferred from the following quasistatic relations at low frequency. For torsion, the shear modulus is $|G^*| = |M^*|L/\phi(0.5\pi r^4)$ and for bending Young's modulus is $|E^*| \approx |M^*|L/0.25\pi r^4\phi$. $|M^*|$ is the applied moment, L is the specimen length, r is its radius, ϕ is the end angular displacement inferred from micrometer calibration of the light detector. At the resonance angular frequencies ω_0 in torsion and bending, damping, $\tan\delta$, was calculated from the width of the dynamic

compliance curve using the width $\Delta\omega$ at half maximum of the curve of dynamic structural compliance θ/M^* according to $\tan\delta \approx (1/\sqrt{3})(\Delta\omega/\omega_0)$. Studies were conducted at ambient temperature, 22°C. Wet specimens were kept wet via a slow drip over a gauze layer surrounding the specimen.

2.2 Bone Specimens. The donor for the bone was a Caucasian male, six feet tall and 135 pounds, who died at age 75 of pneumonia. The bone used was the mid-diaphyseal portion of this man's right tibia. Our decision to test bone specimens taken from a tibia was based on the fact that of the long bones in the human body, the three-sided tibia provides the best site from which a usable-sized ''transverse'' specimen can be taken. The body had been maintained fresh frozen. Bone sections were frozen in individually sealed plastic bags until they were thawed for machining. Freezing appears not to affect mechanical properties of bone significantly [16–18]. One tibia was used in this study since: (*i*) multiple tests over a wide frequency range were time-consuming, and (*ii*) comparison of torsion, bending, longitudinal, transverse, wet, and dry conditions for the same bone was of interest. Two complete series of experiments were conducted for different longitudinal and transverse specimens from this tibia. It is recognized that, given biological variability, a greater number of specimens and bones is desirable. However, owing to the time-consuming nature of these experiments, such study is reserved for the future.

Specimens were rough cut with a band saw, then turned to a diameter of 3 mm using a small table-top lathe. The transverse specimen was 12 mm long. The longitudinal specimen was 17 mm long. One end of each specimen was drilled and tapped to receive a 0-90 screw for attachment to a magnet. After machining, the specimens were either mounted directly into the apparatus while moist with Ringer's solution, or they were frozen while moist with Ringer's solution. An antibacterial agent, ''Complete Remedy'' (Wardley Watercare), an aquarium disinfectant containing 3.3 percent sodium chlorite, was incorporated, one drop per two cups of Ringer's solution, to prevent bone decay. This is greater than the dosage recommended for fish aquariums by a factor of about five. The disinfectant is not considered likely to influence bone properties at concentrations comparable to those tolerable by living fish. No evidence of such influence was evident. After bone specimens had been tested while wet, they were allowed to air dry in the laboratory's ambient environment until their mass ceased changing over time (their moisture content reached equilibrium). They were then tested again in both torsion and bending. There were eight trials involving wet, dry, torsion, bending, longitudinal, and transverse orientation.

Values for shear and Young's moduli of elasticity as well as the resultant maximum strains due to torsion and bending were calculated for the specimen in its wet condition at a driving frequency of 10 Hz. Maximum surface strain was calculated from the observed end angular displacement in torsion and bending. Since applied torque was so small, maximum strain was much less than failure strain. Density was calculated as mass divided by specimen volume as calculated from dimensions. This is referred to as apparent density; porosity was not considered in the calculation.

3 Results

3.1 Modulus and Density. Values for shear and Young's moduli of elasticity as well as the resultant maximum strains due to torsion and bending were calculated for the specimen in its wet condition at a driving frequency of 10 Hz. These calculations were done based on the analytical solution for bending and torsion of a circular cylinder. For the first wet longitudinal specimen, the shear modulus G was 3.42 GPa, Young's modulus E was 12.8 GPa, and the maximum shear and bending strains, γ and ε, were 1.9 and 0.48 μstrain. These strains are well within the ranges for both linear viscoelasticity and physiological loading. Moreover, the moduli and densities are within the accepted normal range for bone. Specifically, Reilly and Burstein [19] deduce for compact bone a range of Young's modulus of 6 to 24 GPa, depending on mineralization, porosity, and method; they measured 17 GPa and a density of 1.8 g/cm^3. As for shear modulus, Reilly and Burstein [19] deduce $G = 3.1$ and 5.4 GPa by other authors; they measured $G = 3.3$ GPa. The wet density of specimen L8 was 1.90 g/cm^3, and its dry density (with relative humidity 55 percent) was 1.81 g/cm^3. Wet density may be converted to water content via the method of Sasaki and Enyo [20].

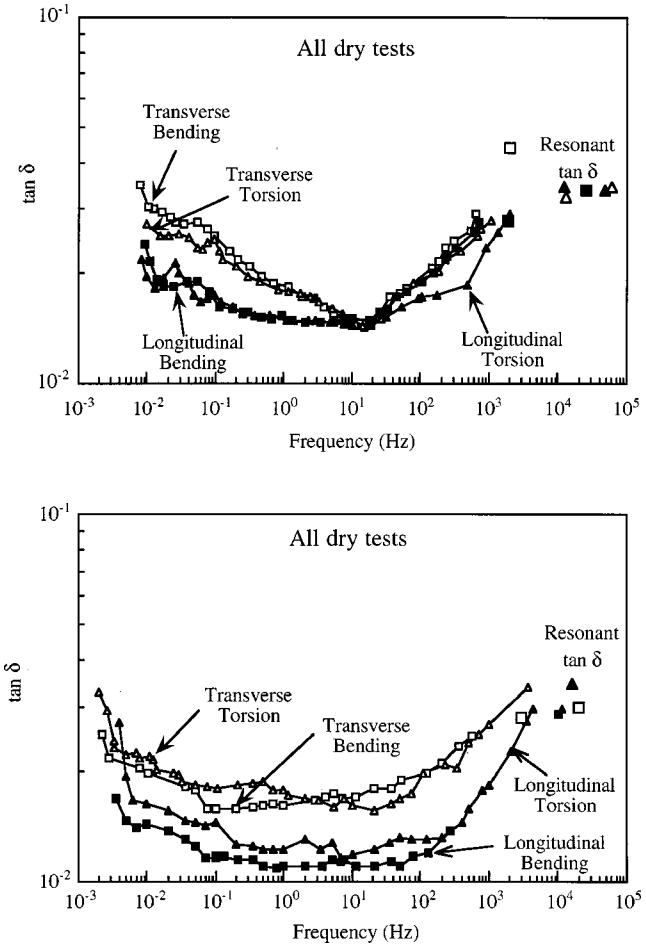

Fig. 3 Comparison of measured tan δ for dry bone, top, first specimen; bottom, second specimen. Torsion: transverse, △; longitudinal, ▲. Bending: transverse, □; longitudinal, ■.

For transverse specimen TA1 when wet, the shear modulus G was 2.7 GPa, Young's modulus E was 9.3 GPa, and the maximum shear and bending strains, γ and ε, were 2.19 and 0.55 μstrain. Wet apparent density was 2.14 g/cm^3, and dry apparent density (with relative humidity of 76 percent) was 2.01 g/cm^3.

3.2 Loss Tangent. Results for $\tan\delta$ versus frequency for the various conditions are shown in Figs. 3–6. For each figure, two sets of plots are given, corresponding to the two sets of specimens. All the plots have in common a relative minimum in $\tan\delta$ over a frequency range predominantly contained in normal activities. A similar minimum is evident in the results in Fig. 1, derived from various authors and bone from different anatomic sites.

The four curves for dry bone (Fig. 3) show similar behavior for the longitudinal bending and torsion results. Transverse bending and torsion results were similar and exhibited higher $\tan\delta$ than longitudinal below 10 Hz. These results are similar for frequencies greater than 10 Hz. Since there is not fluid flow in a dry

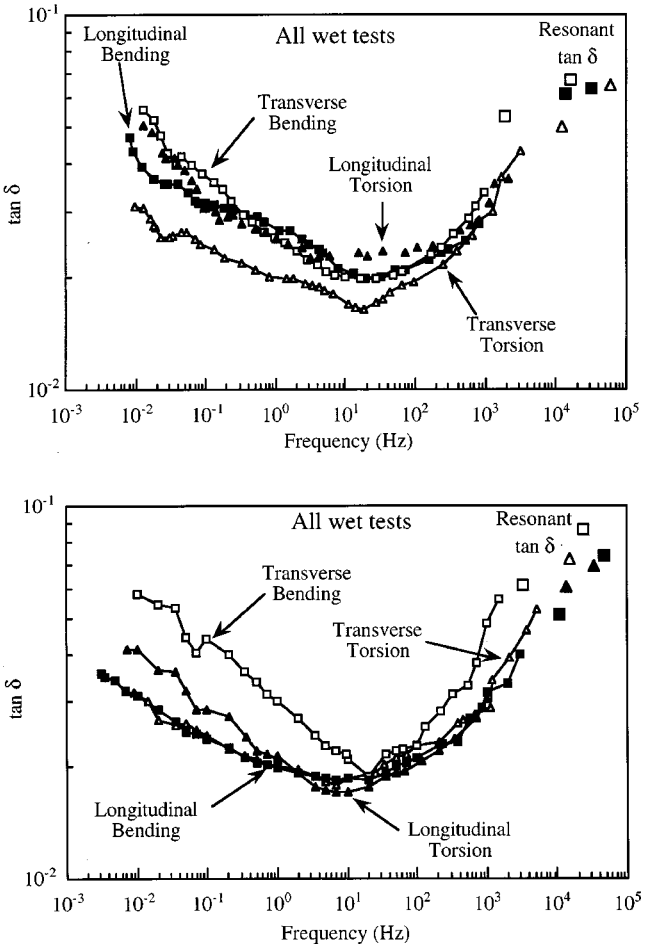

Fig. 4 Comparison of measured tan δ for wet bone, top, first specimen; bottom, second specimen. Torsion: transverse, △; longitudinal, ▲. Bending: transverse, □; longitudinal, ■.

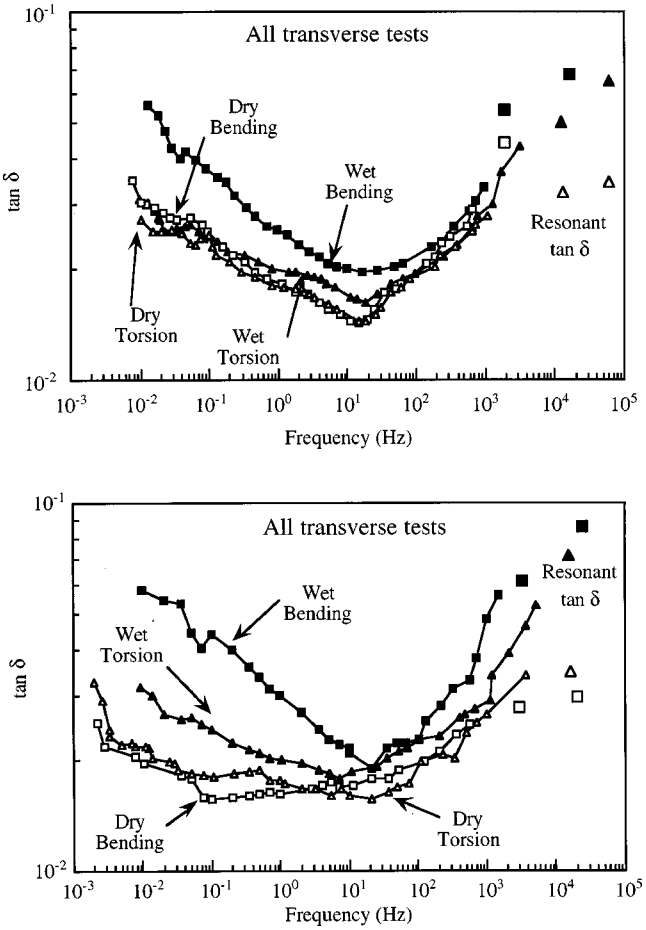

Fig. 5 Comparison of measured tan δ for transverse cut bone, top, first specimen; bottom, second specimen. Torsion: dry, △; wet, ▲. Bending: dry, □; wet, ■.

specimen, differences in damping must come from other causes. The most likely cause is molecular mobility in collagen or in other biopolymers.

The four curves for wet bone (Fig. 4) show similar behavior for all cases except transverse torsion, which exhibited lower damping than the others at the lower frequencies. The difference is substantially greater than the phase resolution of the instrumentation.

The four curves for transverse bone (Fig. 5) show similar behavior above 100 Hz. Below 100 Hz, the results from the wet and dry torsion tests and the dry bending test all are similar, while tan δ for the wet bending test was substantially higher than for the others.

The four curves for longitudinal bone (Fig. 6) show similar behavior in torsion and bending for wet bone and for dry bone; tan δ for wet bone substantially exceeds tan δ for dry bone, particularly below 100 Hz. This trend is different from that observed in Fig. 5 for transverse bone in which only wet bending differed significantly from the others. All wet tan δ results are higher than the corresponding dry tan δ results.

4 Discussion

4.1 Phenomena and Comparisons. All the plots have in common a relative minimum in tan δ over a frequency range predominantly contained in normal activities. These results support the evidence for such a minimum (in Fig. 1), derived from results in shear for bone from various anatomic sites by different authors. This minimum in damping at physiologic frequencies is inconsistent with an optimal shock-absorbing role for bone [21] based on its viscoelastic response, though shock absorption by bone may play some role. As for axial deformation such as occurs in bending, results obtained by various authors [22–27], were converted to a common representation and compared by Lakes and Katz [28]. Their analysis of the axial relaxation results of Lugassy and Korostoff [24] implies tan $\delta \approx 0.015$ at 0.0016 Hz and tan $\delta \approx 0.045$ at 0.016 Hz. This is a reasonable agreement with the current results for bending. By contrast, the axial constant strain rate results of McElhaney [25] imply tan $\delta \approx 0.15$ at 1.6 Hz, an order of magnitude too high. Such stress-strain curves are graphically appealing; nevertheless, they are inconsistent with the present results as well as with other literature. The discrepancy may result from nonlinear viscoelastic behavior not accounted for in the transformation process, from differences in the bone, or from experimental artifacts. Sasaki et al. [2] studied relaxation in bovine femoral bone for times from 10 s to 10^5 s (about one day). The shortest time studied in these tests corresponds to about 0.016 Hz in the frequency domain. Relaxation was similar in torsion and bending, in qualitative agreement with the present results.

Curve fitting of viscoelastic data may employ a single exponential in relaxation $E(t)$ in the time domain,

$$E(t) = E_2 + E_1 e^{-t/\tau_r}, \tag{1}$$

with τ_r as a relaxation time.

The frequency domain response is related to the time domain response by Fourier transformation. The corresponding Debye peak in tan δ in the frequency domain is

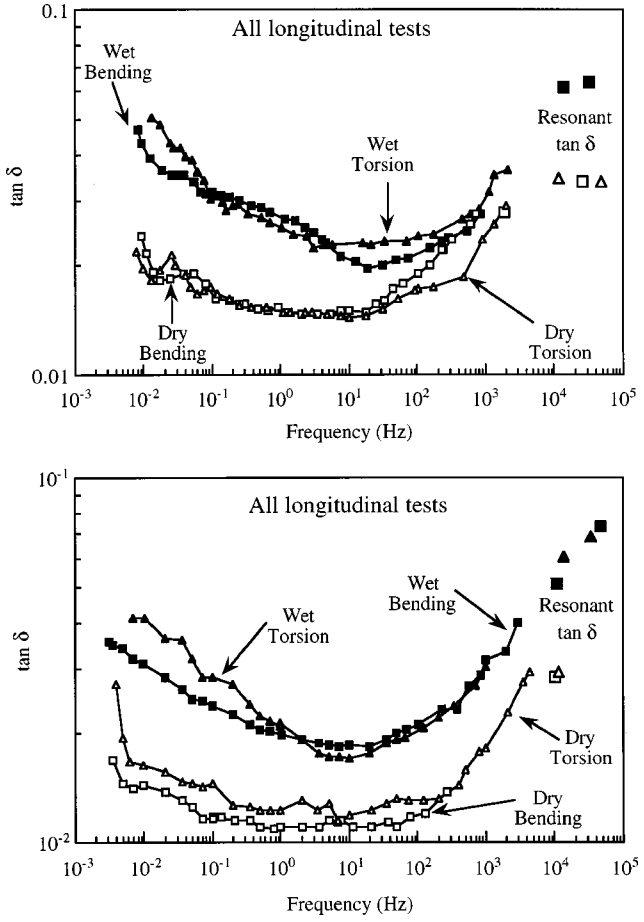

Fig. 6 Comparison of measured tan δ for longitudinal cut bone, top, first specimen; bottom, second specimen. Torsion: dry, △; wet, ▲. Bending: dry, □; wet, ■.

$$\tan\delta(\omega)=\frac{\Delta}{\sqrt{1+\Delta}}\frac{\omega\tau_m}{1+\omega^2\tau_m^2}, \tag{2}$$

with $\tau_m=\tau_r\sqrt{1+\Delta}$ as a time constant, $\omega=2\pi v$ as angular frequency, and v as frequency. A sample Debye peak is shown in Fig. 1. The *relaxation strength* Δ is defined as the change in stiffness during relaxation divided by the stiffness at long time,

$$\Delta=\frac{E(0)-E(\infty)}{E(\infty)}=E_1/E_2. \tag{3}$$

Here $E(\infty)$ is the relaxation modulus at infinite time and $E(0)$ is the relaxation modulus at zero time. For small damping the peak height is tan $\delta\approx\Delta/2$. The observed loss tangent of bone occupies a much larger region of the frequency domain than a Debye peak.

Sasaki et al. [2] fitted their results with a superposition of a stretched exponential or KWW (after Kohlrausch, Williams, Watts) form and a Debye model (Eq. (2)). The KWW form is:

$$E(t)=(E(0)-E(\infty))e^{-(t/\tau_r)^\beta}+E(\infty), \tag{4}$$

with $0<\beta\leqslant 1$, $E(0)$ and $E(\infty)$ as constants, t is time, and τ_r is a characteristic relaxation time.

The dynamic behavior corresponding to the KWW relaxation is tan δ in the form of a broad peak with tan $\Delta\approx v^{-\beta}$ for frequencies v well above the peak. The general increase in tan δ with decreasing frequency below 1 Hz is characteristic of the present results, the results of Lakes et al. [29] and the model of Sasaki et al. [2]. Moreover, a triangle-shaped relaxation spectrum for the long-time region used by Lakes and Katz [6] also gives an increase in tan δ with decreasing frequency. By numerically transforming the Sasaki results for torsion, we obtain tan $\delta\approx 0.0078$ at 10^{-2} Hz, tan $\delta\approx 0.021$ at 10^{-3} Hz, and 0.039 at 10^{-4} Hz. The bovine bone used by Sasaki et al. [2] generally has moderately lower damping than human bone; however, the computed value at 0.01 Hz is significantly lower than values reported here and elsewhere. Since the shortest time in the Sasaki data, 10 s, corresponds to 0.016 Hz, the model cannot be expected to apply at shorter times or lower frequencies than those present in the experimental data. The time constant in the Debye model used by Sasaki et al. [2] in all cases exceeds 10^5 s, the longest time examined. Therefore their curve fit does not provide evidence for existence of a Debye peak. As for hydration, Sasaki and Enyo [20] studied bone viscoelasticity as a function of water content. They found that the slower modes of relaxation became more important as water content increased.

The present results show an increasing tan δ at high frequency. This region of behavior has not been explored previously by others, and is not treated by models such as those of Sasaki et al. [2], which treat long-time, low-frequency behavior.

4.2 Mechanisms. Several causal mechanisms give rise to a single exponential in relaxation or creep, consequently a Debye peak in tan δ. For example, the classical Biot [7] theory predicts that fluid flow in communicating porosity of a single size scale gives rise to such a peak. The magnitude of the expected peak can be evaluated by calculating the relaxation strength Δ (Eq. (3)) associated with the fluid flow process. The width of a Debye peak on a logarithmic frequency scale is shown for comparison with experimental results in Fig. 1.

Tissues actually contain structure, including porosity, with a hierarchical distribution of length scales [3,30], which can give rise to a distribution of relaxation times, most easily surveyed if data over many decades of time or frequency are presented on a logarithmic scale. Haversian canals have diameters of order 70 μm. They comprise the coarse vascular porosity and tend to orient primarily with the longitudinal axes of long bones. The lacunae are roughly ellipsoidal and have dimensions of about $10\times 15\times 25$ μm [31,32], and have a volume fraction of approximately 5 percent in cortical bone. Canaliculi, having a gross volume fraction of approximately 5 percent, are minute channels having diameters of order 0.35 μm. They connect lacunae to each other and ultimately to the vascular porosity [33–35]. The varying length scales and orientations of these porosities can result in anisotropic stiffnesses and fluid conductivities in cortical bone.

To explore the effect of the fluid phase numerically, bone matrix and the roughly cylindrical porosities of Haversian canals were idealized on the microscale as periodic fluid–solid composites and subject finite element unit cell modeling [36]. Figure 7 shows the Haversian bone model. The solid phase was assumed to be linear, isotropic elastic ($E=20.0$ GPa; $G=7.14$ GPa). The fluid

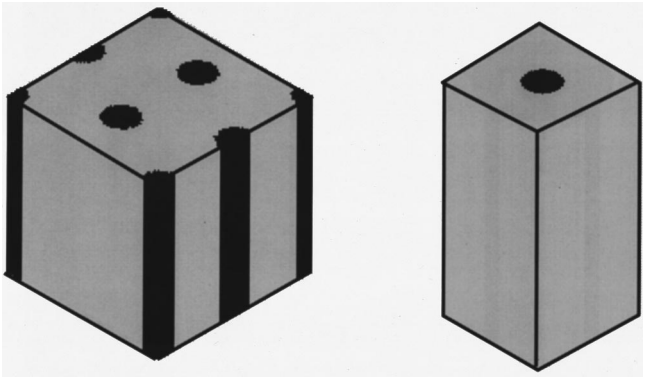

Fig. 7 (*a*) Periodic arrangement of cylindrical canals, representing either Haversian porosity, or canalicular porosity; and (*b*) unit cell of canal and bone matrix

Table 1 Results of unit cell computations on saturated cortical bone model

Longitudinal Loading			Shear		Transverse Loading	
Haversian porosity	undrained El(GPa)	drained El(GPa)	G_{12}(GPa)	G_{23}(GPa)	undrained Etr(GPa)	drained Etr(GPa)
0.00	20.00	20.00	7.142	7.142	20.0	20.0
0.05	18.70	18.69	5.924	6.240	17.15	16.86
0.10	17.60	17.59	5.004	5.584	15.28	14.86
0.15	16.55	16.54	4.114	5.029	13.93	13.42
0.20	15.41	15.39	3.313	4.444	12.43	11.81

phase, having the bulk modulus of water (2.1 GPa), occupied a cylindrical channel within the bone matrix. The unit cell model for varying levels of porosity was subjected to longitudinal and transverse numerical compression tests under both undrained and drained conditions using methods presented in Swan [37].

Some results are shown in Table 1. When bone is stressed longitudinally in an undrained manner, the peak calculated fluid pressure in the Haversian canals are consistently in the range of 2 percent of the applied uniaxial stress. When the bone is stressed uniaxially in an undrained manner in directions transverse to the long axis, calculated peak fluid pressures in the Haversian canals are about 16 percent of the applied stress. To achieve such fluid stresses, it should be re-emphasized that the bone must be stressed quickly enough so as to respond in an undrained fashion, i.e., so rapidly there is no time for the fluid to flow. Since the Haversian porosities treated in these unit cell models are aligned either in the transverse or longitudinal directions, the analysis indicates no fluid pressure buildup when bone is subjected to states of pure shear stress in the principal material coordinates. However, for oblique channels (such as Volksman canals and/or canaliculi) pure shear would indeed lead to buildup of fluid pressures and thus fluid flow. The expected difference in short-term undrained Young's moduli and long-term fully drained Young's moduli of cortical bone when loaded in the longitudinal direction is very modest, even for 20 percent Haversian porosity: $E_{\text{undrained}}/E_{\text{drained}} \approx 1.0013$. For transverse loading, Haversian porosities on the order of 20 percent result in $E_{\text{undrained}}/E_{\text{drained}} \approx 1.05$. Since the unit cell models utilized here do not predict coupling between the fluid and solid phases under pure shear loading, they result in $G_{\text{undrained}}/G_{\text{drained}} = 1$. This unit cell analysis therefore suggests a peak tan δ of bone in longitudinal bending of approximately 0.0006 and a peak tan δ under transverse loading of approximately 0.025. The latter peak is large enough to be easily observable above the background damping from other sources.

As for the frequency and time scale of apparent viscoelasticity in cortical bone due to fluid flow, there appears to be considerable uncertainty. Salzstein and Pollack [38] found pore pressure relaxation times to be on the order of 1 s by measuring the electromechanical potentials associated with applied loads in cortical bone. More recently, Zhang et al. [39] used analytical models to predict that fluid pressures in Haversian porosity relax on time scales of microseconds while fluid pressures in canaliculi relax on time scales of milliseconds, assuming bone fluid viscosity is that of saline water. Stewart [36] used porous medium finite element analysis, with moduli estimated from the preceding unit cell analysis results, and porosities in agreement with those measured by Rouhana et al. [40], to determine that a cortical bone specimen 3 mm in diameter and 17 mm in length should exhibit a peak tan δ in bending near 10 MHz if transversely cut, and near 1 MHz if longitudinally cut. Such frequencies are well beyond those used in the present study.

All tan δ values for all the wet tests were higher than all tan δ values for the corresponding dry tests. In addition to the absence of fluid flow in dry bone, drying also can alter the mobility of groups in the collagen macromolecules in bone. Collagen is a natural fibrous polymer. As with other polymers, viscoelasticity arises due to molecular motions. Wetting of bone may facilitate molecular motions, as a plasticizer facilitates molecular motions in synthetic polymers. Collagen is highly constrained by cross-links and close apposition with mineral crystallites. A broad distribution of tan δ is expected from such a molecular mobility mechanism. By contrast, a fluid flow related damping process would give rise to a Debye peak, about one decade (a factor of ten) wide in the frequency domain. That is provided there is only one length scale associated with the fluid filled channels (i.e., Haversian canals or canaliculi, but not both). The role of the fluid within the matrix itself is currently unknown. Even so, since expected behavior from macroscopic fluid flow differs so much from molecular mechanisms, it is of interest to use air-dried bone as a control.

No obvious Debye peaks are evident in the present results. Among the transverse results in Fig. 5, tan δ is highest for the wet condition in bending. Such behavior is qualitatively consistent with the results of the finite element predictions, but the elevation in tan δ is considerably broader than a Debye peak, which covers only about one decade. The expected peak may have been broadened (and thus decreased in height) due to the variety of pore sizes present in bone. It is also possible that due to the small specimen size and relatively high permeability, the peak in tan δ might be at a high frequency, 1 to 10 MHz [36] above those accessible in this study. If the peak occurs at such high frequencies, then fluid flows freely in response to physiological mechanical stresses, and no pressure buildup occurs in the Haversian systems.

While viscoelasticity at the lowest frequencies was attributed to viscous-like motion at the cement lines by Lakes and Saha [4], the cause of the increase of viscoelasticity at the highest frequencies has not been identified. Lakes et al. [41] considered fluid flow in connection with ultrasonic effects in bone; however, in this study we observed increasing damping with frequency in both wet and dry bone. The damping cannot, therefore, be primarily due to fluid flow. A molecular mechanism of the organic portion of the bone is suggested. The rise in damping at high frequency is characteristic of a rubbery material. It is possible that molecules or molecular groups have the degree of mobility found in rubbery polymers. The ground substance at the cement line boundaries may be considered as a candidate region these molecules might occupy.

5 Conclusions

Human cortical bone exhibits a greater tan δ when wet than when dry. All the results have in common a relative minimum in tan δ over a frequency range, 1 to 100 Hz, which is predominantly found in normal activities. The observed minimum in damping is inconsistent with a shock-absorbing role for bone [21] based on its viscoelastic response. Over the frequency range studied, there is no definitive evidence of a damping peak that could be attributed to fluid flow. If, as suggested by finite element analysis, the peak indeed occurs above 100 kHz, then fluid flows freely in response to physiological mechanical stresses, and no pressure buildup occurs in the Haversian systems.

Acknowledgments

The authors are grateful for a grant from the Whitaker Foundation.

References

[1] Rauber, A. A., 1876, ''Elasticität und Festigkeit der Knochen. Anatomisch–Physiologische Studie,'' Engelmann, Leipzig.

[2] Sasaki, N., Nakayama, Y., Yoshikawa, M., and Enyo, A., 1993, ''Stress Relaxation Function of Bone and Bone Collagen,'' J. Biomech., **26**, pp. 1369–1376.

[3] Katz, J. L., 1980, ''Anisotropy of Young's Modulus of Bone,'' Nature (London), **283**, pp. 106–107.

[4] Lakes, R. S., and Saha, S., 1979, ''Cement Line Motion in Bone,'' Science, **204**, pp. 501–503.

[5] Lakes, R. S., and Katz, J. L., 1979, ''Viscoelastic Properties of Wet Cortical Bone: Part II, Relaxation Mechanisms,'' J. Biomech., **12**, pp. 679–687.

[6] Lakes, R. S., and Katz, J. L., 1979, ''Viscoelastic Properties of Wet Cortical Bone: Part III, A Non-linear Constitutive Equation,'' J. Biomech., **12**, pp. 689–698.

[7] Biot, M. A., 1941, ''General Theory of Three-Dimensional Consolidation,'' J. Appl. Phys., **12**, pp. 155–164.

[8] Djerad, S. E., Du Burck, F., Naili, S., and Oddou, C., 1992, ''Analyze du Comportement Rhéologique Instationnaire d'un Echantillon de Muscle Cardiaque,'' C. R. Acad. Sci. Paris, Série II, **315**, pp. 1615–1621.

[9] Piekarski, K., and Munro, M., 1977, ''Transport Mechanism Operating Between Blood Supply and Osteocytes in Long Bones,'' Nature (London), **269**, pp. 80–82.

[10] Cowin, S. C., 1993, ''Bone Stress Adaptation Models,'' ASME J. Biomech. Eng., **115**, pp. 528–533.

[11] Cowin, S. C., Weinbaum, S., and Zeng, Y., 1995, ''A Case for Bone Canaliculi as the Anatomical Site of Strain Generated Potentials,'' J. Biomech., **28**, No. 11, pp. 1281–1297.

[12] Cowin, S. C., 1998, ''On the Calculation of Bone Pore Water Pressure Due to Mechanical Loading,'' Int. J. Solids Struct., **35**, Nos. 34–35, pp. 4981–4997.

[13] Chen, C. P., and Lakes, R. S., 1989, ''Apparatus for Determining the Properties of Materials Over Ten Decades of Frequency and Time,'' J. Rheol., **338**, pp. 1231–1249.

[14] Brodt, M., Cook, L. S., and Lakes, R. S., 1995, ''Apparatus for Measuring Viscoelastic Properties Over Ten Decades: Refinements,'' Rev. Sci. Instrum., **66**, pp. 5292–5297.

[15] Lakes, R. S., and Quackenbush, J., 1996, ''Viscoelastic Behaviour in Indium Tin Alloys Over a Wide Range of Frequency and Time,'' Philos. Mag. Lett., **74**, pp. 227–232.

[16] Stromberg, L., and Dalen, N., 1976, ''The Influence of Freezing on the Maximum Torque Capacity of Long Bones, An Experimental Study on Dogs,'' Acta Orthop. Scand., **47**, No. 3, pp. 254–256.

[17] Hamer, A. J., Strachan, J. R., Black, M. M., Ibbotson, C. J., Stockley, I., and Elson, R. A., 1996, ''Biomechanical Properties of Cortical Allograft Bone Using a New Method of Bone Strength Measurement—A Comparison of Fresh, Fresh-Frozen and Irradiated Bone,'' J. Bone Joint Surg. Br., **78B**, pp. 363–368.

[18] Kang, Q., An, Y., and Friedman, R. J., 1997, ''Effects of Multiple Freezing-Thawing Cycles on Ultimate Indentation Load and Stiffness of Bovine Cancellous Bone,'' Am. J. Vet. Res., **58**, pp. 1171–1173.

[19] Reilly, D. T., and Burstein, A. H., 1975, ''The Elastic and Ultimate Properties of Compact Bone Tissue,'' J. Biomech., **8**, pp. 393–405.

[20] Sasaki, N., and Enyo, A., 1995, ''Viscoelastic Properties of Bone as a Function of Water Content,'' J. Biomech., **28**, pp. 809–815.

[21] Paul, I. L., Munro, M. B., Abernethy, P. J., Simon, S. R., Radin, E. L., and Rose, R. M., 1978, ''Musculo-Skeletal Shock Absorption: Relative Contribution of Bone and Soft Tissues at Various Frequencies,'' J. Biomech., **11**, pp. 237–239.

[22] Black, J., and Korostoff, E., 1973, ''Dynamic Mechanical Properties of Viable Human Cortical Bone,'' J. Biomech., **16**, p. 435.

[23] Currey, J. D., 1965, ''Anelasticity in Bone and Echinoderm Skeletons,'' J. Exp. Biol., **43**, p. 279.

[24] Lugassy, A. A., and Korostoff, E., 1969, ''Viscoelastic Behavior of Bovine Femoral Cortical Bone and Sperm Whale Dentin,'' in: *Research in Dental and Medical Materials*, Plenum, NY.

[25] Mcelhaney, J. H., 1966, ''Dynamic Response of Bone and Muscle Tissue,'' J. Appl. Physiol., **21**, pp. 1231–1236.

[26] Smith, R., and Keiper, D., 1965, ''Dynamic Measurement of Viscoelastic Properties of Bone,'' Am. J. Med. Electron, **4**, p. 156.

[27] Tennyson, R. C., Ewert, R., and Niranjan, V., 1972, ''Dynamic Viscoelastic Response of Bone,'' Experim. Mech., **12**, p. 502.

[28] Lakes, R. S., and Katz, J. L., 1974, ''Interrelationships Among the Viscoelastic Functions for Anisotropic Solids: Application to Calcified Tissues and Related Systems,'' J. Biomech., **7**, pp. 259–270.

[29] Lakes, R. S., Katz, J. L., and Sternstein, S. S., 1979, ''Viscoelastic Properties of Wet Cortical Bone—I. Torsional and Biaxial Studies,'' J. Biomech., **12**, pp. 657–678.

[30] Lakes, R. S., 1993, ''Materials With Structural Hierarchy,'' Nature (London), **361**, pp. 511–515.

[31] Cooper, R. R., Milgram, J. W., and Robinson, R. A., 1966, ''Morphology of the Osteon: An Electron Microscopic Study,'' J. Bone Joint Surg., **48A**, pp. 1239–1271.

[32] Hancox, N. M., 1972, *Biology of Bone*, Cambridge University Press.

[33] Frost, H. M., 1963, *Bone Remodeling Dynamics*, Charles C. Thomas, Springfield, IL.

[34] Pope, M. H., and Outwater, J. H., 1972, ''Fracture Initiation in Compact Bone,'' ASME Paper No. 72-WA/BHF-3.

[35] Kufahl, R. H., and Saha, S., 1990, ''Canaliculi-Lacunae Network,'' J. Biomech., **23**, pp. 171–180.

[36] Stewart, K. J., 1999, ''Deformation Induced Fluid Flow as a Mechanism for Bone Adaptation,'' M.S. thesis, University of Iowa, Iowa City, IA.

[37] Swan, C. C., 1994, ''Techniques for Stress- and Strain-Controlled Homogenization of Inelastic Periodic Composites,'' Comput. Methods Appl. Mech. Eng., **117**, pp. 249–267.

[38] Salzstein, R. A., and Pollack, S. R., 1987, ''Electromechanical Potentials in Cortical Bone—II. Experimental Analysis,'' J. Biomech., **20**, pp. 271–280.

[39] Zhang, D., Weinbaum, S., and Cowin, S. C., 1998, ''Estimates of Peak Pressures in Bone Pore Water,'' ASME J. Biomech. Eng., **120**, pp. 697–703.

[40] Rouhana, S. W., Johnson, M. W., Chakkalakal, D. A., Harper, R. A., and Katz, J. L., 1981, ''Permeability of Compact Bone,'' Joint ASME–ASCE Conference of the Biomechanics Symposium, ASME AMD-Vol. 43 pp. 169–172.

[41] Lakes, R. S., Yoon, H. S., and Katz, J. L., 1983, ''Slow Compressional Wave Propagation in Wet Human and Bovine Cortical Bone,'' Science, **220**, pp. 513–515.

[42] Thompson, G., 1971, ''Experimental Studies of Lateral and Torsional Vibration of Intact Dog Radii,'' Ph.D. thesis, Biomedical Engineering, Stanford University.

[43] Lakes, R. S., 1982, ''Dynamical Study of Couple Stress Effects in Human Compact Bone,'' ASME J. Biomech. Eng., **104**, pp. 6–11.

[44] Adler, L., and Cook, C. V., 1975, ''Ultrasonic Parameters of Freshly Frozen Dog Tibia,'' J. Acoust. Soc. Am., **58**, pp. 1107–1108.

[45] Park, H. C., and Lakes, R. S., 1986, ''Cosserat Micromechanics of Human Bone: Strain Redistribution by a Hydration-Sensitive Constituent,'' J. Biomech., **19**, pp. 385–397.